Formation of DNA toroids inside confined droplets adsorbed on mica surfaces

Xi-Miao Hou, Wei Li, Shuo-Xing Dou, Ling-Yun Zhang, Ping Xie, Wei-Chi Wang, and Peng-Ye Wang*
Laboratory of Soft Matter Physics, Beijing National Laboratory for Condensed Matter Physics, Institute of Physics, Chinese Academy of Sciences, Beijing 100190, China

(Received 1 January 2009; revised manuscript received 17 March 2009; published 18 May 2009)

We report observations of *in vitro* DNA compaction into toroids in the absence of any condensing agent. The DNA toroid formation is induced by geometry confinement from microdroplets on mica surfaces. With AFM imaging we show that the confined DNA molecules may take the form of random coils or semiordered folded loops with large microdroplets, while they readily take the form of compact and ordered toroids when the microdroplet sizes are small enough. To better understand these phenomena, we carried out coarse-grained Brownian dynamics simulation, obtaining results that were in good agreement with the experimental observations. The simulation reveals that the toroid formation is sensitive to not only the microdroplet size, but also the DNA stiffness.

DOI: 10.1103/PhysRevE.79.051912 PACS number(s): 87.14.gk, 07.79.Lh, 87.15.ap, 87.15.hp

DNA generally exists in condensed state in all living organisms. Especially, in viruses and most vertebrate sperm cells DNA is packed into a rather compact and ordered structure with a strikingly decreased size [1]. Condensed DNA has also potential applications in gene therapy [2]. The mechanisms underlying various DNA condensation phenomena are still not understood very well. Among all the different DNA condensations, toroid represents a fundamental morphology for high density packing [3]. Previous studies have discovered several kinds of *in vitro* DNA condensing agents that can induce DNA condensations to toroids similar to those in bacteriophage capsids. These agents generally make DNA to condense in the following several ways. (a) Decreasing repulsions between DNA segments by neutralizing the phosphate's negative charge by multivalent cations such as spermidine, cobalt hexamine, and basic proteins such as H1 and protamine [4]; (b) making DNA-solvent interactions less favorable by poor solvent such as ethanol [5]; (c) excluding volume to DNA by crowding agents such as polymer PEG [6]. However differently from toroid formations by condensing agents *in vitro*, packing of DNA into virus occurs through the geometry confinement by the protein capsid and an ATP-driven motor [7,8].

We report in this work another way for DNA toroid formation: geometry confinement. As will be described below, the geometry confinement here resulted from microdroplets formed through quick contraction of liquid layers on mica surface when blown by nitrogen flow. We find that with the decrease in microdroplet size, DNA configuration changes from random coils to semiordered folded loops, and finally to toroids. DNA cannot be packed illimitably. We also carried out theoretical work to simulate the condition of DNA in confined spaces. The results were in good agreement with the experimental observations. This kind of DNA compaction should be useful for studying the intrinsic properties of DNA and especially for understanding the principle of virus packing: packing of the DNA genome into a preformed protein capsid requires DNA to be highly compressed, with the aid of an ATP-driven motor [7,8], into a small space comparative to its persistence length, resembling the present DNA compaction by geometry confinements.

In the experiments, the 2-kb double-stranded DNA fragments were produced by polymerase chain reaction (PCR) using λ-DNA as a template and 5′-TGGTCGTTCAGGGTTGTCGGA-3′ and 5′-CGCCTTGCCCTCGTCTATGTA-3′ as primer sequences. The DNA was purified by gel extraction and then dissolved in 10 mM Tris-HCl buffer with pH 7.5. All samples for AFM observation were prepared in the same way. First, add Mg^{2+} to DNA solution with a final concentration of 5 mM. Next, deposit a 10 μL droplet of the solution onto a newly cleaved mica surface. Then, after an adsorption for 5 min, gently rinse the surface by slowly dropping 200 μL deionized water onto it, then absorbing the solution away to leave only a thin layer. Finally, dry the mica surface with a nitrogen flow. The last step was crucial for making the sample. The optimum condition at a temperature of 22 °C was that the relative humidity of air was between 20%–30% (i.e., a dry environment), under which the liquid adhered, through hydrophilic interaction, to the mica surface might quickly shrink locally into microdroplets with the nitrogen blowing. Depending on the flow rate of nitrogen, the microdroplet diameters ranged from ~50 to ~800 nm and, when the nitrogen flow was too strong, no microdroplet was formed. After formation, the microdroplets were allowed to dry naturally without further nitrogen flow. Then the samples were scanned in air by the tapping mode with a Nanoscope IIIa AFM.

As just mentioned, when nitrogen flow was strong, microdroplets could not be formed, because the thin layer of liquid on the mica surface receded quite rapidly and completely. In this case, the DNA molecules appeared in relaxed and extended natural configurations on the mica surface, with a height of ~0.7 nm [see Fig. 1(a)]. We call them free DNA, which means that DNA molecules are not confined by microdroplets.

With reduced nitrogen flow, microdroplets would form readily on the mica surfaces. Since Mg^{2+} provided only weak binding between DNA and the mica surface [9], allowing DNA to diffuse in two dimensions on mica surface, DNA

*pywang@aphy.iphy.ac.cn

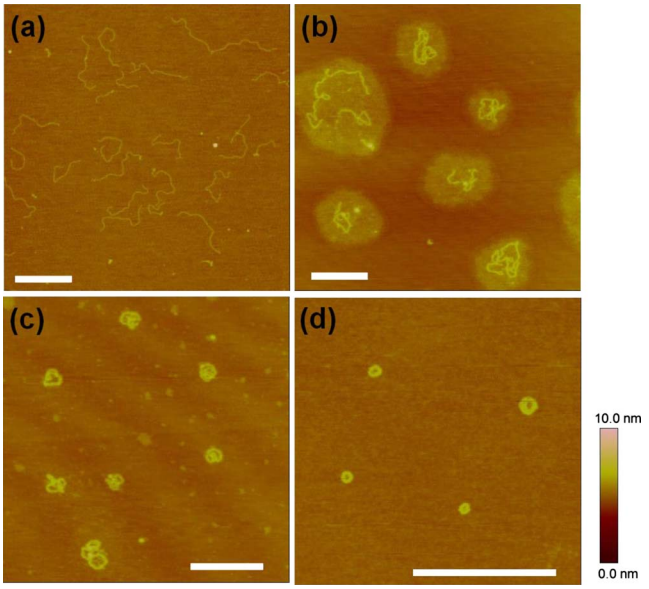

FIG. 1. (Color online) Different morphologies of 2-kb DNA on mica surfaces as observed by AFM. The nitrogen flow rate used was decreased sequentially in the four cases. (a) Free and extended DNA. (b) DNA confined within about 400–800 nm ranges. (c) Semiordered DNA structures with sizes of ~150 nm. (d) DNA toroids with ordered structure. All scale bars are 500 nm.

molecules moved readily with the buffer and thus would be confined into the microdroplets. The biggest microdroplets in our experiments were about 800 nm in diameter. After the microdroplet formation, we stopped the flow of nitrogen and let the liquid in the microdroplets to sufficiently evaporate for several hours. Then with AFM, we could see the conformations of the confined DNA.

In the case of Fig. 1(b) where the microdroplets were large (400–800 nm), the DNA molecules still coiled flexibly. But when compared with their natural configurations [Fig. 1(a)], they appeared to be slightly restricted in size. We call them disordered DNA. It is worth to note that since mica surface was hydrophilic, the liquid evaporated slowly from the whole surface of the microdroplets without contracting their boundaries, as clearly shown in Fig. 1(b). This indicates that the microdroplet diameters on mica were fixed at time of drying with nitrogen flow. As the microdroplets were large, more than one DNA molecules were frequently trapped within a single microdroplet.

When the microdroplets were formed with a size of about 150 nm, most DNA molecules appeared as folded close loops [Fig. 1(c)]. We call them semiordered DNA. In this case, the DNA molecules were obviously highly restricted within the microdroplets and thus they preferred to locate near the microdroplet boundaries, in contrast with the previous case in Fig. 1(b). In most cases, only one DNA molecule was trapped within each microdroplet.

When the nitrogen flow was slow, very small microdroplets would be formed and the liquid inside them evaporated instantly in the process of blowing with nitrogen. Surprisingly, in such cases, DNA were highly compressed and packed into toroids with appearances similar to that formed by multivalent cations [10,11] [Fig. 1(d)]. This is an observation of *in vitro* DNA toroids formation without using any condensing agent.

We have also used 1-kb double-stranded DNA (produced by PCR from λ-DNA) in the experiments and obtained similar results. In addition, we found that a variation in Mg^{2+} concentration from 1 to 5 mM did not change the results. Intuitively, the smallest toroid sizes should be correlated with a balance between the maximum confinement force produced by the microdroplets and the elasticity of the strained DNA.

DNA toroids formed by multivalent ions such as spermidine and cobalt hexamine are reported to be around 100 nm in the outside diameter and 30 nm in the inside diameter. This size is independent of DNA molecular length from 400 to 40 000 bp and many molecules may be included in a single toroid [12]. The present toroids formed by geometry confinement [Fig. 1(d)] are smaller and thinner (the diameter and height averaged for 77 toroids are about 50 and 2 nm, respectively). Each toroid is comprised of a single 2-kb DNA molecule in most cases. In addition, the condensation process by geometry confinement is more rapid, nearly instantaneously with the blowing of nitrogen.

We also investigated the effect of divalent cations on toroid formation. If no cation was used, no DNA would be observed on mica surface, indicating that DNA needed to be adsorbed to the mica surface, at least not repulsed by it. When Ni^{2+} was used, DNA was strongly adsorbed, and was unable to be packed, consistent with the fact that the transition metal cations helped to bind DNA effectively to mica surface [13]. Therefore, divalent cation is needed to bind DNA to mica, but the binding should not be too strong to prevent compaction. Mg^{2+} properly provides the loose connection between DNA and the mica surface. In fact, Allen *et al.* [4] reported that when DNA was first adsorbed onto mica surface loosely and then protamine was added as condensing agent, toroids structures could be observed. Besides, rinsing mica surface with anhydrous ethanol after DNA molecules have been adsorbed loosely onto mica could also produce toroids [5]. These two kinds of DNA condensation are both directed by surfaces. Similarly, the DNA compaction in our work occurs after DNA adsorption onto mica surface weakly by Mg^{2+}, so we guess the process may also be assisted by the surface. Considering that Mg^{2+} cannot only attach DNA molecules to mica surface, but also induce DNA condensation when dielectric constant of the solution is reduced by addition of alcohol [14,15], it is possible that Mg^{2+} may play a role in driving the coil to toroid transition, although very small amount of Mg^{2+} would remain in the solution left on mica surface due to the rinse of the surface.

From the above results, we see that with the decrease in microdroplet size, the DNA structures changed from being disordered (random coils) to semiordered (folded close loops) and finally to highly ordered (toroids). This size effect phenomenon reminds us what happens in virus packing: when 20% DNA is packed into capsid, the slightly restricted DNA differs little from free DNA as random coils; when 55%–60% DNA is packed, the main highly ordered pattern is formed, and remains conserved until the packing completion [16].

Next, we performed the same experiments with full-length λ-DNA. Figure 2(a) shows the long free DNA mol-

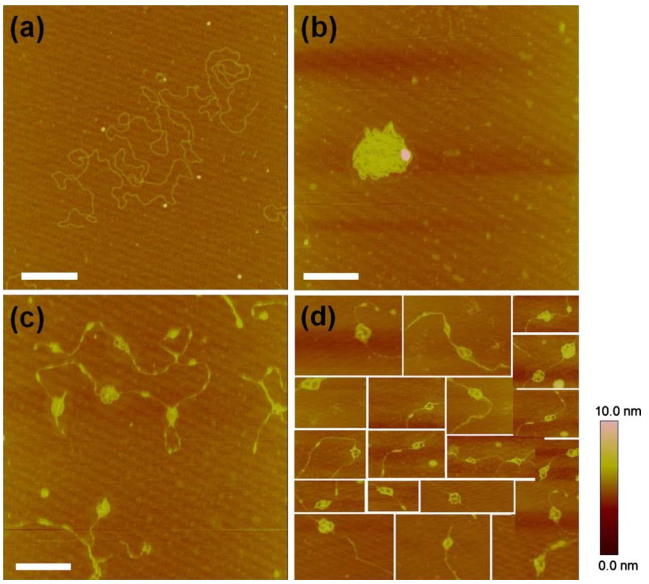

FIG. 2. (Color online) Different morphologies of λ-DNA on mica surfaces as observed by AFM. The nitrogen flow rate used was decreased sequentially in the four cases. (a) Free and extended DNA adsorbed onto the surface. (b) DNA completely compressed into disordered structures. (c) DNA in partially compressed structures. (d) Selected semiordered structures or ordered DNA toroids. All scale bars are 500 nm.

ecules curled randomly on the mica surface, without any geometry confinement. In the case of microdroplet formation, DNA might be completely trapped in microdroplets and thus compressed to disordered structures [Fig. 2(b)]. More frequently, the long DNA molecules were not completely trapped in microdroplets and thus were only partially compressed to disordered structures [Fig. 2(c)]. When the microdroplets were small enough (on the order of several tens of nanometers), the compressed portions of DNA might show semiordered or even ordered toroid structures [Fig. 2(d)], similar to the case of DNA fragments [Figs. 1(c) and 1(d)]. When the genome is fully packed, the pressure inside the λ-phage wall reaches a very high value (about 50 atm) as a result of DNA bending and pushing against the phage wall, as well as DNA-DNA electrostatic repulsion [17–20]. If the surface tension of the microdroplet cannot bear this high pressure, DNA strand will come out. This explains why λ-DNA is unable to be confined by the droplet into a single toroid in our experiments.

To better understand the DNA compaction phenomena described above, we performed numerical simulation by coarse-grained Brownian dynamics. A water microdroplet was modeled as a spherical cap inside which a DNA chain was trapped. By reducing the microdroplet size, we study how the DNA conformation changes.

In the simulation, the DNA is modeled as a semiflexible homopolymer chain, which consists of N spheres connected by bonds. Each sphere corresponds to a length of about 6 bp DNA. The potentials of the system are considered as follows.

The self-avoiding effect of DNA chain is considered by using the repulsive part of the Morse potential,

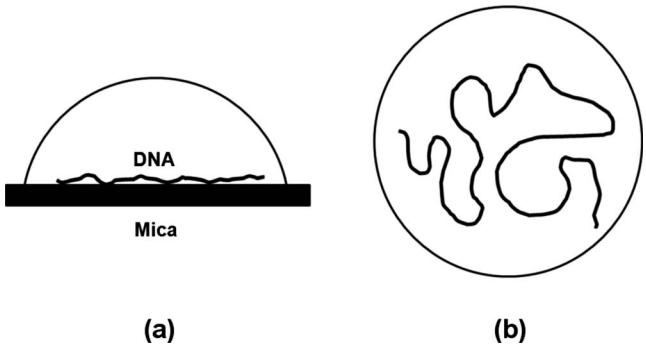

FIG. 3. A schematic representation of the system consisting of the water microdroplet, DNA, and mica. (a) Side view; (b) top view.

$$\frac{U_{m,rep}}{k_BT} = \varepsilon_m \sum \exp\{-\alpha_m(r_{i,j} - \sigma_m)\}, \tag{1}$$

where ε_m=0.1, α_m=2.4, and σ_m is the width of DNA. k_B is the Boltzmann constant and the temperature T=300 K. $r_{i,j}$ is the distance between the ith and jth spheres of the DNA chain. σ_m is the equilibrium distance between two neighboring spheres of the DNA chain. We use σ_m as the length unit (6 bp DNA).

The bonds between neighboring spheres of the DNA chain are considered through a harmonic bonding potential,

$$\frac{U_{bond}}{k_BT} = \frac{k}{2\sigma_m^2} \sum (|\vec{r}_i - \vec{r}_{i+1}| - \sigma_m)^2, \tag{2}$$

where k=400, $\vec{r}_i$ and $\vec{r}_{i+1}$ are the location vectors of the ith and $(i+1)$th spheres of the DNA chain. We model the chain stiffness by using the bending potential,

$$\frac{U_{bend}}{k_BT} = \kappa \sum \left(1 - \frac{(\vec{r}_{i-1} - \vec{r}_i) \cdot (\vec{r}_i - \vec{r}_{i+1})}{\sigma_m^2}\right), \tag{3}$$

where we choose κ=25.

The weak binding between DNA and the mica surface due to Mg^{2+} is considered by Morse potential,

$$\frac{U_{m,mica}}{k_BT} = \varepsilon \sum [\exp\{-2\alpha(R_i - \sigma)\} - 2\exp\{-\alpha(R_i - \sigma)\}], \tag{4}$$

where ε=0.1, α=6.0, σ=0.5σ_m and R_i is the distance between the ith spheres of DNA chain and mica surface.

The overdamped Langevin equation is used to describe the motion of each DNA sphere,

$$-\gamma_m \frac{d\vec{r}_i}{dt} + \vec{R}_{m,i}(t) - \frac{\partial U}{\partial \vec{r}_i} + \vec{F}_{st} = 0, \tag{5}$$

where γ_m is the friction constants of the DNA sphere, which is calculated according to Stokes law. $\vec{R}_{m,i}$ is the Gaussian white noises which obey the fluctuation-dissipation theorem. The total internal energy U consists of three terms: $U = U_{m,rep} + U_{bond} + U_{bend} + U_{m,mica}$. $\vec{F}_{st}$ is surface tension for DNA segment touching water surface and is calculated according to $F_{st} = 2\gamma l$, where γ is chosen as

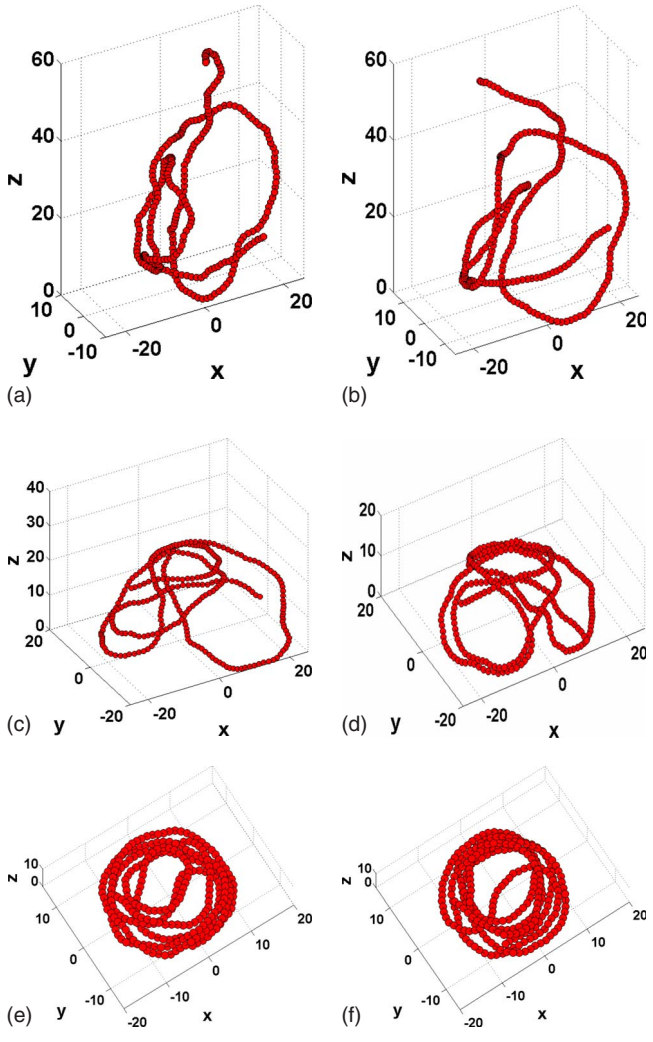

FIG. 4. (Color online) The dynamics of DNA compaction by geometry confinement. The volume corresponding to each snapshot is as follows: (a) 2.28×10^6, (b) 5.98×10^5, (c) 4.75×10^4, (d) 5.18×10^3, (e) 1.41×10^3, and (f) 9.38×10^2 (length unit^3). The initial radius and height of the modeled water microdroplet are 109 and 105 length unit and the final values are 12 and 4 length unit. For clarity, we have not shown the water microdroplet.

71.97×10^{-3} N/m and l is the length of the DNA segment.

We perform the dynamics by using the first-order Ermak-McCammon algorithm [21,22]:

$$d\vec{r}_i = \frac{D_i}{k_B T}\vec{f}_i dt + \sqrt{2D_i dt}\,\vec{\omega}_i, \tag{6}$$

where $D_i = k_B T/\gamma_m$ is the diffusion coefficient, $\vec{\omega}_i$ is a random noise vector obtained from a standard normal distribution, and $\vec{f}_i = -\nabla U + \vec{F}_{st}$.

We first calculate a free DNA chain consisting of 300 DNA spheres (about 1800 bp in total). The persistence length of the model DNA is about 49.2 nm (κ=25), which is consistent with that of natural DNA under normal solution conditions [23,24]. Then, we put the DNA chain into a spherical cap water microdroplet where the DNA molecule is confined

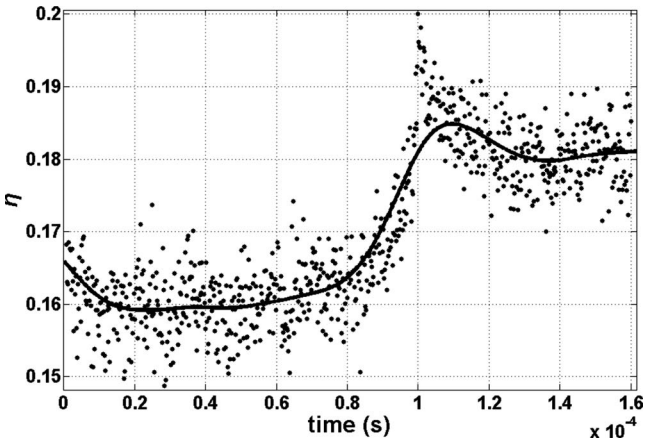

FIG. 5. The change in parameter η during the process of DNA compaction by geometry confinement. Volume corresponding to the jump is close to the final volume 9.38×10^2 (length unit^3).

by the microdroplet surface while constrained weakly onto the mica surface by Mg^{2+} (Fig. 3), and change the spherical cap's size continually. The dynamical process is shown in Fig. 4. With decreasing water microdroplet size, the free and

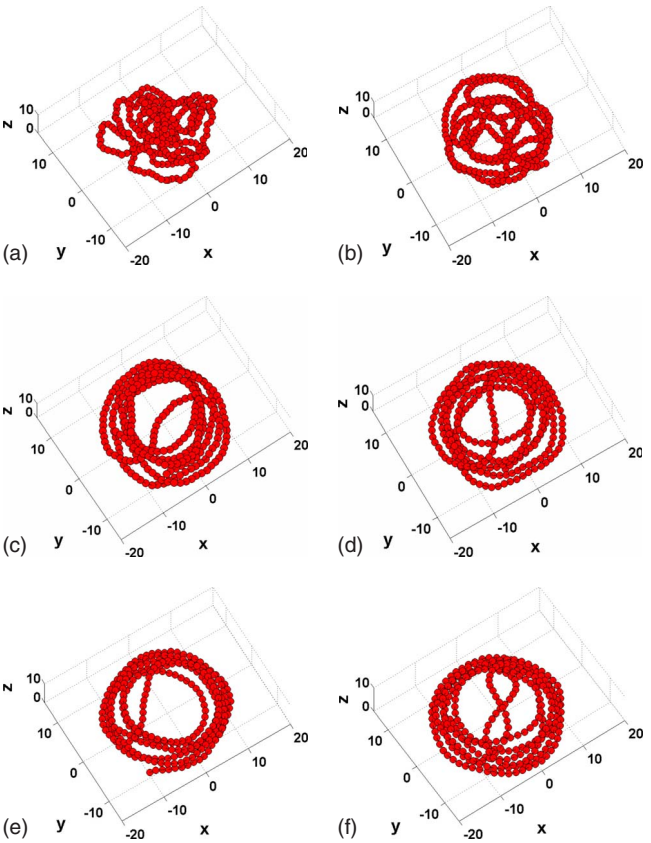

FIG. 6. (Color online) We change the DNA chain stiffness parameter κ to check the effect of persistence length on DNA's self-organization. The radius and height of the modeled microdroplet are fixed, respectively, at 12 and 4 length unit. The value of κ corresponding to each picture is as follows: (a) 5, (b) 15, (c) 25, (d) 30, (e) 35, and (f) 40.

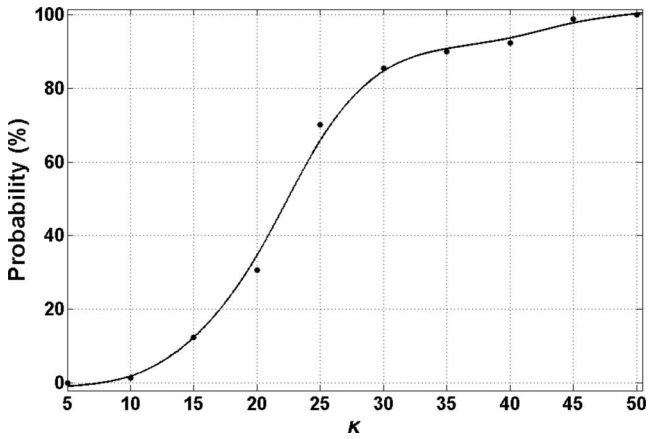

FIG. 7. Probability of forming ordered toroid structures versus the DNA chain stiffness parameter κ. The radius and height of the modeled microdroplet are fixed, respectively, at 12 and 4 length unit. For each point, we repeat the simulations for 20 times.

disordered DNA is gradually compressed to an ordered toroid structure due to geometry confinement.

We introduce parameter η as a measure of the structural order of the DNA chain:

$$\eta = \frac{\left|\sum \vec{r}_{i,i+1} \times \vec{r}_{i+1,i+2}\right|}{N-2}, \tag{7}$$

where N is number of DNA spheres. In the ordered structure, the directions of most neighboring vectors are generally parallel to each other and the value of η becomes larger. During the DNA compaction process (Fig. 4), the parameter η changes in the way as shown in Fig. 5. The jump of η at $\sim 1 \times 1.0^{-4}$ s corresponds to the change in DNA from disordered to ordered structures.

Persistence length is an important parameter characterizing the intrinsic stiffness of DNA. To check the effect of persistence length on the DNA compaction, we changed the stiffness parameter κ used in describing the DNA bending potential U_{bend} in Eq. (3) and made the simulations repeatedly to obtain the probability of forming ordered toroid structures at different κ (Fig. 6). As expected, when the DNA chain is soft (i.e., small κ), the probability is low, but when the DNA chain is stiff enough, DNA always takes the form of an ordered toroid (Fig. 7).

In a similar way, we studied the effect of microdroplet size on the toroid formation by obtaining the probability of forming ordered toroid structures at varying microdroplet radius (Fig. 8). As shown in Fig. 9, the toroid formation is sensitive to the microdroplet size, in agreement with the experimental observations in Fig. 1.

In summary, we present our experimental and theoretical work on *in vitro* DNA compaction induced by geometry confinement from microdroplets. The formation of microdroplets is a result of temperature, humidity, and the nitrogen flow. We observe that when the microdroplet is small enough to exert strong confinement to DNA, the DNA may take the form of ordered toroids. Theoretical modeling has been developed that can reproduce the structural features of the confined DNA. The modeling indicates that the persistence length of DNA and the microdroplet size are both important

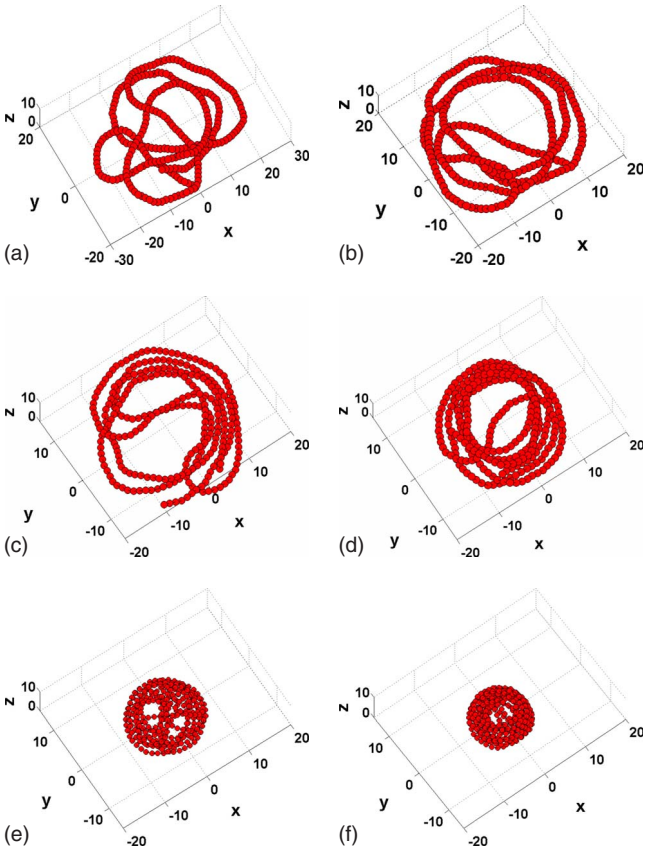

FIG. 8. (Color online) We change the final microdroplet radius to check the effect of microdroplet size on DNA's self-organization. The height of the water microdroplet is fixed at 4 length unit and the stiffness parameter κ is 25. The microdroplet radius corresponding to each picture is as follows: (a) 24, (b) 20, (c) 16, (d) 12, (e) 9, and (f) 5.

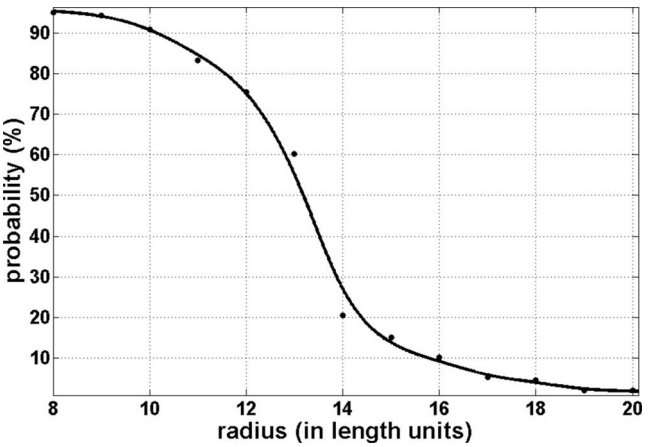

FIG. 9. Probability of forming ordered toroid structures versus the microdroplet radius. The height of the water microdroplet is fixed at 4 length unit and the stiffness parameter κ is 25. For each point, we repeat the simulations for 20 times.

for the compact toroid formation. This phenomenon of *in vitro* packing of DNA to toroids in the absence of any condensing agent may be used for further studies of virus packing mechanism and for developments of new gene therapy techniques.

This research was supported by the National Natural Science Foundation of China (Grants No. 10834014, No. 10674173, and No. 30770517) and the National Basic Research Program of China (973 Program) (Grant No. 2009CB930704).

[1] V. A. Bloomfield, Biopolymers **44**, 269 (1997).
[2] M. Schmutz, D. Durand, A. Debin, Y. Palvadeau, A. Etienne, and A. R. Thierry, Proc. Natl. Acad. Sci. U.S.A. **96**, 12293 (1999).
[3] N. V. Hud and K. H. Downing, Proc. Natl. Acad. Sci. U.S.A. **98**, 14925 (2001).
[4] M. J. Allen, E. M. Bradbury, and R. Balhorn, Nucleic Acids Res. **25**, 2221 (1997).
[5] C. Zhang and Johan R. C. van der Maarel, J. Phys. Chem. B **112**, 3552 (2008).
[6] L. S. Lerman, Proc. Natl. Acad. Sci. U.S.A. **68**, 1886 (1971).
[7] D. E. Smith, S. J. Tans, S. B. Smith, S. Grimes, D. L. Anderson, and C. Bustamante, Nature (London) **413**, 748 (2001).
[8] M. C. Williams, Proc. Natl. Acad. Sci. U.S.A. **104**, 11125 (2007).
[9] G. Zuccheri, R. T. Dame, M. Aquila, I. Muzzalupo, and B. Samori, Appl. Phys. A **66**, S585 (1998).
[10] M. R. Shen, K. H. Downing, R. Balhorn, and N. V. Hud, J. Am. Chem. Soc. **122**, 4833 (2000).
[11] C. C. Conwell, I. D. Vilfan, and N. V. Hud, Proc. Natl. Acad. Sci. U.S.A. **100**, 9296 (2003).
[12] V. A. Bloomfield, Biopolymers **31**, 1471 (1991).
[13] H. G. Hansma and D. E. Laney, Biophys. J. **70**, 1933 (1996).
[14] V. A. Bloomfield, Curr. Opin. Struct. Biol. **6**, 334 (1996).
[15] R. W. Wilson and V. A. Bloomfield, Biochemistry **18**, 2192 (1979).
[16] A. S. Petrov and S. C. Harvey, Structure **15**, 21 (2007).
[17] S. Tzlil, J. T. Kindt, W. M. Gelbart, and A. Ben-Shaul, Biophys. J. **84**, 1616 (2003).
[18] J. Kindt, S. Tzlil, A. Ben-Shaul, and W. M. Gelbart, Proc. Natl. Acad. Sci. U.S.A. **98**, 13671 (2001).
[19] A. Evilevitch, L. Lavelle, C. M. Knobler, E. Raspaud, and W. M. Gelbart, Proc. Natl. Acad. Sci. U.S.A. **100**, 9292 (2003).
[20] A. Evilevitch, J. W. Gober, M. Phillips, C. M. Knobler, and W. M. Gelbart, Biophys. J. **88**, 751 (2005).
[21] D. L. Ermak, J. Chem. Phys. **62**, 4189 (1975).
[22] D. L. Ermak and J. A. McCammon, J. Chem. Phys. **69**, 1352 (1978).
[23] J. Moukhtar, E. Fontaine, C. Faivre-Moskalenko, and A. Arneodo, Phys. Rev. Lett. **98**, 178101 (2007).
[24] J. A. Schellman, Biophys. Chem. **11**, 321 (1980).